Attosecond pulse generation using high harmonics in the multicycle regime of the driver pulse

Fam Le Kien,* Katsumi Midorikawa, and Akira Suda
The Institute of Physical and Chemical Research (RIKEN), Hirosawa 2-1, Wako-shi, Saitama 351-0198, Japan
(Received 24 February 1998)

High-harmonic generation in He atoms illuminated by high-intensity femtosecond excitation pulses is studied. It is shown that single attosecond pulses as well as trains of several attosecond pulses, one per half a period, can be generated in the multicycle regime of the driver pulse. [S1050-2947(98)06910-8]

PACS number(s): 42.65.Ky, 42.65.Re, 32.80.Rm, 42.50.Hz

I. INTRODUCTION

In recent years there have been very significant advances in short-pulse high-intensity laser technology. The discovery of high-order harmonic generation by intense laser-atom interaction provides a new method to produce coherent extreme-ultraviolet emission. Coherent x rays in the water window have been generated using high harmonics [1,2]. The durations of extreme-ultraviolet femtosecond high-harmonic pulses have been measured by a cross-correlation technique [3]. The nonadiabatic effects in high-harmonic generation with ultrashort pulses have been examined [4]. The phase-matching conditions for optimal coherence of high harmonics emitted by atoms in strong laser fields have been studied [5,6].

One of the recent topics of high-harmonic generation is its potential application to the generation of attosecond pulses. Since the time scale for a Bohr orbit of ground-state hydrogen is about 152 attoseconds, it is expected that attosecond pulses will expand the horizon of ultrafast measurements to include observing electronic processes. Several schemes for the generation of light pulses in the attosecond regime have been proposed. Hänsch has proposed a Fourier synthesizer [7] that can generate subfemtosecond pulses by superposition of equidistant frequencies from separate laser oscillators synchronized by a nonlinear phase-locking technique. Farkas and Tóth [8] have suggested a method of attosecond light pulse generation that is based on a Fourier synthesis of equidistant high harmonics. Harris *et al.* [9] have shown that a strongly driven classical oscillator in a soft Coulomb potential will exhibit short bursts of acceleration and consequently produce ultrashort pulses of radiation. Corkum *et al.* have suggested the use of two short perpendicularly polarized pulses [10] to create a laser pulse whose polarization is linear only during a short time, close to a laser period. Due to the high sensitivity of harmonic generation to the degree of polarization ellipticity, the emission will be limited to this interval and, therefore, an attosecond pulse will be generated. The production of a train of several attosecond pulses per half cycle and the selection of one pulse from this train by propagation have been numerically demonstrated by Antoine *et al.* [11]. Schafer and Kulander have shown that the high harmonics emitted when a nonlinear medium interacts with an ultrafast intense laser pulse are, in principle, compressible to subfemtosecond time scales [12]. The high-harmonic generation of attosecond pulses in the single-cycle regime has been studied by Christov *et al.* [13]. A scheme using a laser pulse with a time-dependent degree of ellipticity and including propagation has been investigated by Antoine *et al.* [14].

A simple picture of underlying physics in high-harmonic emission has been given by Corkum [15] and Kulander *et al.* [16] using a semiclassical approach. In this picture, an intense laser pulse ionizes the outer electron of an atom by suppressing the Coulomb barrier binding the electron to the atom, so that the electron can tunnel through the core potential. Once free, the electron moves in the laser field and gain a kinetic energy. When the laser field reverses, the electron can reencounter the parent ion, and emit high harmonics if it undergoes stimulated recombination with the parent ion.

An analytic quantum theory of high-harmonic generation has been suggested by Lewenstein *et al.* [17]. This theory recovers the semiclassical interpretation [15,16] and allows us to calculate the harmonic spectrum.

We use this simple analytical quantum model [17] in the present paper to study the generation of high harmonics from He atoms illuminated by high-intensity femtosecond excitation pulses. In order to understand the single-atom aspects clearly, we do not consider the propagation of the generated harmonic field in the nonlinear medium. We show that single attosecond pulses as well as trains of several attosecond pulses, one per half a period, can be generated in the multicycle regime of the driver pulse by performing the Fourier synthesis of the frequency components in relatively regular regions of the harmonic spectrum.

The paper is organized as follows. In Sec. II we review the model and present the basic equations. In Sec. III we perform a numerical analysis. Finally, Sec. IV contains conclusions.

II. MODEL

We consider an atom or an ion in the single-electron approximation under the influence of a laser field $\mathbf{E}(t)$. In atomic units, which we use for all calculations in this paper, the Schrödinger equation takes the form

$$i\frac{d}{dt}|\Psi(\mathbf{r},t)\rangle=[-\tfrac{1}{2}\nabla^2+V(\mathbf{r})+\mathbf{E}(t)\cdot\mathbf{r}]|\Psi(\mathbf{r},t)\rangle. \quad (1)$$

Here, $V(\mathbf{r})$ is the effective potential of the outer electron with respect to the nucleus. We assume that the system is

*Permanent address: Department of Physics, University of Hanoi, Hanoi, Vietnam.

initially in the ground state, denoted as $|0\rangle$, which in general has a spherical symmetry. The peak amplitude E_0 of the electric field is related to the peak intensity I_0 by $I_0=E_0^2$. We consider the case when the ionization potential I_p is very large compared to the laser-field photon energy ω and the ponderomotive energy $U_p=E_0^2/4\omega^2$ is comparable to or larger than I_p, that is, when $U_p \geqslant I_p \gg \omega$. In this regime, the electron undergoes tunneling transitions to the continuum states $|\mathbf{v}\rangle$, which we label by the kinetic momentum $\mathbf{v}$ of the outgoing electron. We assume that the contribution of all bound states except the ground state $|0\rangle$ to the evolution of the system can be neglected. In the continuum, we treat the electron as a free particle moving in the electric field with no effect of $V(\mathbf{r})$.

In order to calculate the time-dependent dipole moment, we have to evaluate $\mathbf{r}(t)=\langle\Psi(\mathbf{r},t)|\mathbf{r}|\Psi(\mathbf{r},t)\rangle$. According to the theory of Lewenstein *et al.* [17], we have

$$\mathbf{r}(t)=-i\int_0^t dt'\int d^3\mathbf{p}\,\mathbf{E}(t')\cdot\mathbf{d}(\mathbf{p}+\mathbf{A}(t')) \times\exp[-iS(\mathbf{p},t,t')]\exp[-\gamma(t)-\gamma(t')]\mathbf{d}^*(\mathbf{p}+\mathbf{A}(t)) +\text{c.c.}, \tag{2}$$

where

$$\mathbf{d}(\mathbf{v})=\langle\mathbf{v}|\mathbf{r}|0\rangle$$

is the atomic dipole matrix element for the bound-free transition,

$$\mathbf{A}(t)=-\int dt\,\mathbf{E}(t) \tag{3}$$

is the vector potential of the laser field,

$$S(\mathbf{p},t,t')=\int_{t'}^t dt''\left\{\frac{1}{2}[\mathbf{p}+\mathbf{A}(t'')]^2+I_p\right\} \tag{4}$$

is the quasiclassical action, and $\gamma(t)$ is the ionization rate. For all calculations in this paper, the ionization rate $\gamma(t)$ is assumed to be a real function of time and is numerically estimated by using the Ammosov-Delone-Krainov (ADK) formula [18]

$$2\gamma(t)=W_{\mathrm{ADK}}\equiv\left(\frac{3e}{\pi}\right)^{3/2}\frac{Z^2}{n^{*9/2}}\left[\frac{4eZ^3}{n^{*4}|\mathbf{E}(t)|}\right]^{2n^*-3/2} \times\exp\left[-\frac{2Z^3}{3n^{*3}|\mathbf{E}(t)|}\right], \tag{5}$$

where Z is the charge of the atomic residue and $n^*=Z(2I_p)^{-1/2}$ is the effective principal quantum number.

Equation (2) can be interpreted as a sum of probability amplitudes corresponding to the following processes: The first term $\mathbf{E}(t')\cdot\mathbf{d}(\mathbf{p}+\mathbf{A}(t'))$ in the integral is the probability amplitude for the electron to make a transition to the continuum at time t' with the canonical momentum $\mathbf{p}$. The electronic wave function is then propagated until time t and acquires a phase factor given by the term $\exp[-iS(\mathbf{p},t,t')]$. The depletion of the ground state is described by the term $\exp[-\gamma(t)-\gamma(t')]$. The electron recombines at time t with an amplitude equal to the last term $\mathbf{d}^*(\mathbf{p}+\mathbf{A}(t))$ of the integral.

In the case of hydrogenlike ground states, the field-free dipole matrix elements can be approximated by [17]

$$\mathbf{d}(\mathbf{p})=i\frac{2^{7/2}\alpha^{5/4}}{\pi}\frac{\mathbf{p}}{(\mathbf{p}^2+\alpha)^3} \tag{6}$$

with $\alpha=2I_p$.

The integral over $\mathbf{p}$ in Eq. (2) can be evaluated by the saddle-point method. The result is

$$\mathbf{r}(t)=-i\int_0^t d\tau\left(\frac{\pi}{\epsilon+i\tau/2}\right)^{3/2}\mathbf{E}(t-\tau)\cdot\mathbf{d}(\mathbf{p}_s+\mathbf{A}(t-\tau)) \times\exp[-iS_s(t,\tau)-\gamma(t)-\gamma(t-\tau)]\mathbf{d}^*(\mathbf{p}_s+\mathbf{A}(t)) +\text{c.c.} \tag{7}$$

Here, we have introduced the notation

$$\mathbf{p}_s=-\frac{1}{\tau}\int_{t-\tau}^t dt''\mathbf{A}(t'') \tag{8}$$

and

$$S_s(t,\tau)=S(\mathbf{p}_s,t,t-\tau), \tag{9}$$

whereas ϵ is a positive regularization constant.

The harmonic amplitude $\mathbf{a}_q$ is obtained by Fourier transforming the time-dependent dipole acceleration $\mathbf{a}(t)$:

$$\mathbf{a}_q=\frac{1}{T}\int_0^T\mathbf{a}(t)e^{iq\omega t}dt. \tag{10}$$

Here $\mathbf{a}(t)\equiv\ddot{\mathbf{r}}(t)$ is the dipole acceleration and T is the duration of the fundamental pulse. We apply a spectral filter to select only the high frequency components starting from harmonic $q_{\min}$ to harmonic $q_{\max}$ and then apply an inverse transform. The intensity of the signal emitted by this synthesis is given by

$$I(t)=\left|\int_{q_{\min}}^{q_{\max}}\mathbf{a}_q e^{-iq\omega t}dq\right|^2. \tag{11}$$

We will use the above model to calculate the emission spectrum and the Fourier synthesis of the spectral components. It has been shown by Antoine *et al.* [11] that, although the harmonics in the plateau region are not strictly speaking phase locked, the time-dependent single-atom emission consists of a train of ultrashort pulses, with several pulses per half cycle, corresponding to various energetically allowed electron trajectories giving rise to harmonic emission. Due to the interference between these trajectories, the emission spectrum is highly structured. The interference is minimal in the spectrum part, which is more or less regular. Therefore, we expect that the Fourier synthesis of a relatively regular part of the spectrum may select a single narrow pulse per half cycle.

III. NUMERICAL RESULTS

We will consider the situation when the laser electric field is linearly polarized along the z direction. We denote the z components of the vectors $\mathbf{E}(t)$, $\mathbf{A}(t)$, and $\mathbf{p}_s$ by $E(t)$, $A(t)$, and p_s, respectively. We study the case when the field with a time-dependent envelope is given as

$$E(t)=E_0\sin^2\left(\frac{\pi t}{T}\right)\cos\omega t. \tag{12}$$

The vector potential then reads

$$A(t)=\frac{E_0}{4}\left(\frac{\sin\omega_- t}{\omega_-}+\frac{\sin\omega_+ t}{\omega_+}-2\frac{\sin\omega t}{\omega}\right), \tag{13}$$

where $\omega_-\equiv\omega-2\pi/T$ and $\omega_+\equiv\omega+2\pi/T$. When we insert the above expression into Eq. (8), we find

$$p_s=-\frac{1}{\tau}[F(t)-F(t-\tau)], \tag{14}$$

where

$$F(t)=\frac{E_0}{4}\left(2\frac{\cos\omega t}{\omega^2}-\frac{\cos\omega_- t}{\omega_-^2}-\frac{\cos\omega_+ t}{\omega_+^2}\right). \tag{15}$$

The value of the quasiclassical action at the saddle point reads

$$S_s(t,\tau)=(I_p-\tfrac{1}{2}p_s^2)\tau+\tfrac{1}{2}[G(t)-G(t-\tau)], \tag{16}$$

where

$$\begin{aligned}G(t)=\frac{E_0^2}{16}\Bigg\{&\left(\frac{1}{2\omega_-^2}+\frac{1}{2\omega_+^2}+\frac{2}{\omega^2}\right)t\\&-\frac{\sin 2\omega_- t}{4\omega_-^3}-\frac{\sin 2\omega_+ t}{4\omega_+^3}-\frac{\sin 2\omega t}{\omega^3}\\&+\frac{1}{\omega_+\omega_-}\left[\frac{\sin(\omega_+-\omega_-)t}{\omega_+-\omega_-}-\frac{\sin(\omega_++\omega_-)t}{\omega_++\omega_-}\right]\\&-\frac{2}{\omega\omega_-}\left[\frac{\sin(\omega-\omega_-)t}{\omega-\omega_-}-\frac{\sin(\omega+\omega_-)t}{\omega+\omega_-}\right]\\&-\frac{2}{\omega\omega_+}\left[\frac{\sin(\omega-\omega_+)t}{\omega-\omega_+}-\frac{\sin(\omega+\omega_+)t}{\omega+\omega_+}\right]\Bigg\}.\end{aligned} \tag{17}$$

We perform numerical calculations for He atoms, whose ionization potential is $I_p=24.58$ eV. We consider the cases when the driver fields are generated by the Ti:sapphire and KrF lasers.

A. Ti:sapphire laser driver field

In this subsection, we use the Ti:sapphire laser for the generation of the driver field. The wavelength and the period of the driver pulse are 794 nm and 2.65 fs, respectively.

We first consider the case when the peak intensity is 1.4×10^{15} W/cm^2. We show in Fig. 1 the power spectrum $|\mathbf{a}_q|^2$ in the $\log_{10}$ scale for the cases when the duration of the driver pulse is 4 (a) and 16 (b) optical cycles. In femtoseconds, the duration of the driver pulse is 10.6 (a) and 42.4 (b) fs. A fractional ionization of 4.5% (a) and 17% (b) is reached at the peak of the driver pulse. We see the characteristic shape of the high-harmonic spectra: they fall off for the first few well-resolved odd harmonics, then exhibit a plateau, and end up with a sharp cutoff. The dip in the front of the plateau occurs at the harmonic order I_p/ω, which is the ionization potential in the unit of the photon energy and is approximately equal to 16 in the case considered. The cutoff occurs at the harmonic order $(I_p+3.17U_p)/\omega$, which is the energy, in the unit of ω, gained by the electron after tunneling and oscillating in the driver laser field, and is approximately equal to 180 in the case considered.

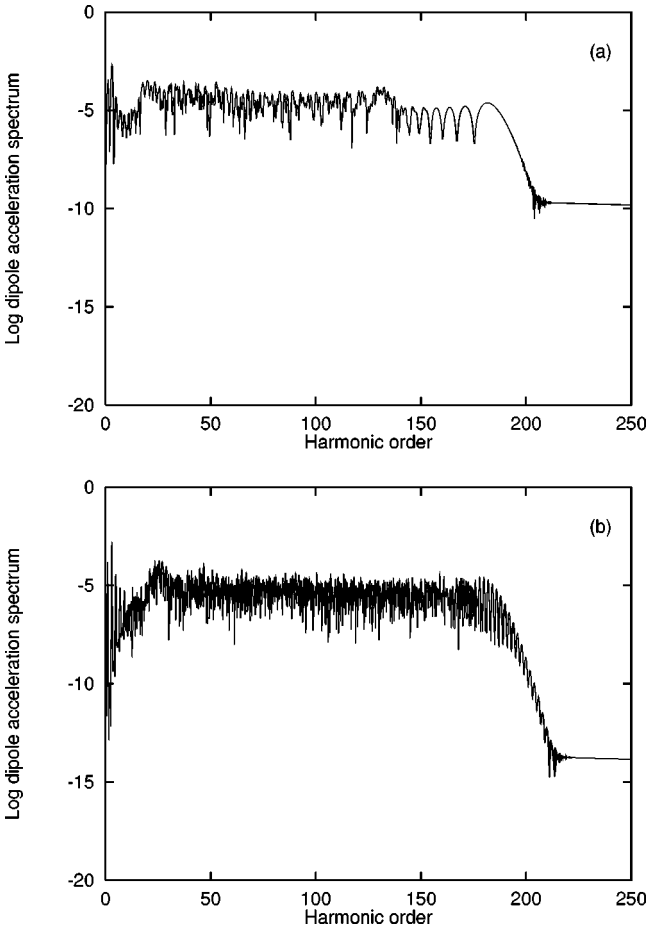

FIG. 1. Power spectral densities ($\log_{10}$ scale) of the dipole acceleration of helium illuminated by the Ti:sapphire laser field with the wavelength 794 nm and the peak intensity 1.4×10^{15} W/cm^2. The duration of the driver field is 4 and 16 optical cycles in the cases (a) and (b), respectively.

As a typical feature of the short-pulse regime, there is a complicated structure with broadening of the peaks and noise between the peaks in the plateau region. Moreover, a supercontinuum near the cutoff occurs in the case of Fig. 1(a), where the pulse duration is 4 optical cycles. The observed broadening of the harmonics is due to the rapid change in the driver-pulse intensity. An electron that enters the continuum while the pump intensity is increasing or decreasing experiences an additional acceleration or deceleration and, consequently, radiates with blueshift or redshift, respectively, after returning to recombine with the parent ion. Since the har-

monics in the plateau are produced over many optical cycles, they have a broad range of frequency shifts and undergo large phase distortions. This explains why the spectrum below the vicinity of the cutoff is highly structured. Since the harmonics at the end of the plateau are produced only during a few cycles near the peak of the driver pulse, they undergo a simple broadening in the short-pulse regime; see Fig. 1(b). This broadening results in a supercontinuum near the cutoff when the driver pulse is very short; see Fig. 1(a).

It is worth noting that the effect of the nonadiabatic atomic response on the low-order harmonics is weaker than on high-order harmonics. Unlike the high-order harmonics, the low-order harmonics with energies smaller than the ionization potential cannot be described by the two-step model [15,16]. The lowest harmonics are emitted due to the trajectories corresponding to the case when the electron remains in the ground state but experiences the near-to-node areas of the laser field. The acceleration of the electron moving along these trajectories is small. This is why the broadening of the lowest harmonics is small and simple compared to that of the high harmonics.

Comparison between Figs. 1(a) and 1(b) shows that the high harmonics are stronger when the driver pulses are shorter. Furthermore, the plateaus of the harmonic spectra consist of several spectral bands separated by sharp drops in the harmonic intensity. Christov *et al.* [13] have shown that the spectral components of the bands are generated during different parts of optical cycles of the laser pulse. They have found that the harmonic generation by a very short pulse ensures a good correspondence between the frequency and time evolution of the harmonic emission. This effect can be used to control the properties of the high harmonics and to generate attosecond pulses. It has been shown [13] that, by separating an appropriate spectral band with filters or broadband mirrors, single attosecond pulses can be emitted in the single-cycle regime of the driver laser field. We will apply this method to the case of multicycle driver pulses.

We use a spectral filter to select only the frequency components in the spectrum part between the 175th and 200th harmonics, which is relatively regular and near the end of the plateau, and then apply an inverse transform. These high frequency components are produced due to the electron trajectories that pass through the peaks of the pump pulse with brief bursts of acceleration. The time dependences of the intensities of the generated frequency-superposition pulses are plotted in Fig. 2. Here we use, for convenience, the relative time calculated from the moment at which the driver pulse reaches its peak. Clearly, the 4-cycle driver pulse produces a single 150-attosecond signal pulse, see Fig. 2(a), while the 16-cycle pulse generates a train of attosecond pulses, one per half a period of the fundamental pulse; see Fig. 2(b). The number of generated attosecond signal pulses decreases when we decrease the number of optical cycles of the driver field.

In the arbitrary units which are the same for both the Figs. 2(a) and 2(b), we calculate the areas of the generated pulses. The area of the single pulse in Fig. 2(a) is 1.67. The area of the highest pulse in Fig. 2(b) is 2.80. When we normalize the areas of the generated pulses to the driver-pulse length, which is proportional to the pump energy, we find that the relative energy conversion efficiencies for the highest pulses

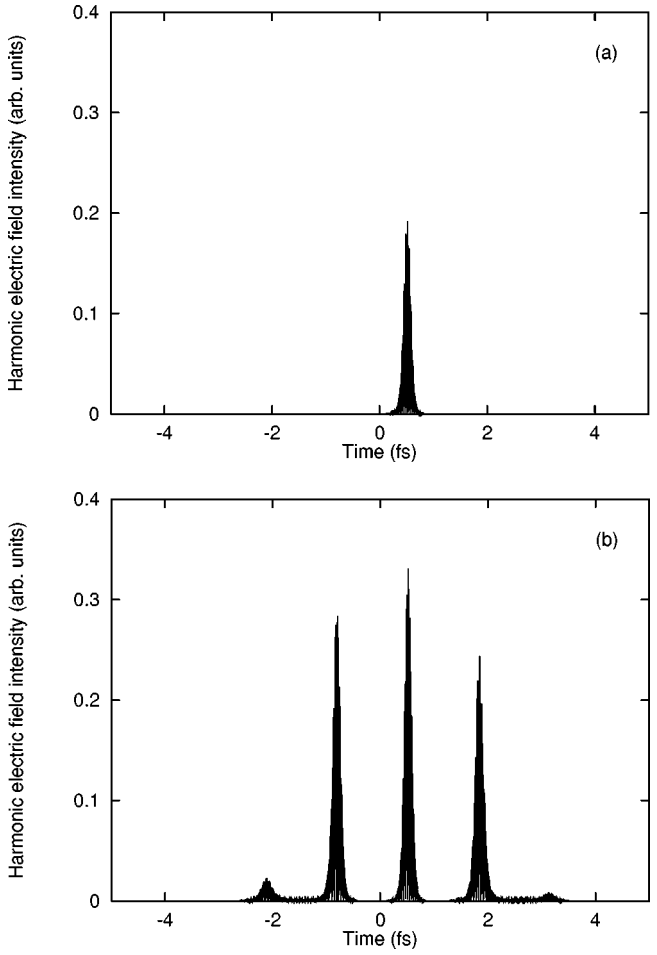

FIG. 2. Time dependencies of the intensities of the superpositions of the spectral components in the bands between the 175th and 200th harmonics of the power spectra shown in Fig. 1.

in Figs. 2(a) and 2(b) are 1:0.42. Thus, the energy conversion efficiency of the highest pulse in each generated train increases when we decrease the number of optical cycles of the driver field.

We can also generate attosecond pulses by combining the low-order frequency components in front of the plateau. We show in Fig. 3 the time development of the radiation obtained by the Fourier synthesis of the frequency components in the relatively regular spectrum region between the 5th and 10th harmonics of the spectrum in Fig. 2(a). The figure shows the generation of a train of attosecond pulses. Due to the small size and the sharp peak structure of the spectrum region between the 5th and 10th harmonics in comparison with the region between the 175th and 200th harmonics, the amplitudes of the pulses in Fig. 3 are much lower than those in Fig. 2(a). Furthermore, the behavior of the optical oscillations of the pulses in Fig. 3 is less regular than that of the pulses in Fig. 2(a). It should be emphasized here that in the region of low-order harmonics, where the parameters of Fig. 3 have been chosen, the theory of Lewenstein *et al.* [17] is a crude approximation; there exist differences between the Lewenstein model and the exact numerical solution of the Schrödinger equation. These differences are due to the fact that the effect of the Coulomb potential in the Lewenstein model is simply reduced to the ionization potential. However, since the Coulomb potential is not completely ne-

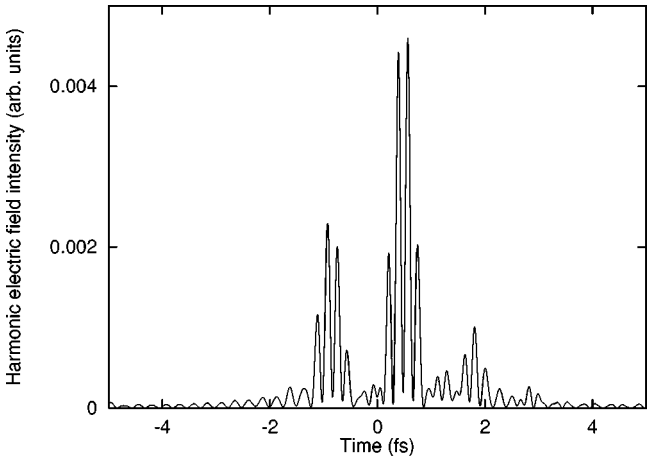

FIG. 3. Time dependence of the intensity of the superposition of the spectral components in the band between the 5th and 10th harmonics of the power spectrum in Fig. 1(a).

glected, the Lewenstein model is able to give a reasonable description of the high-order harmonic spectrum and some principal features of the low-order harmonic region.

The generation of the above attosecond pulses is based on the synthesis of a band of frequencies. These short pulses correspond to the main trajectories of the electron [11]. The phase locking, which plays an essential role in the synthesis of equidistant frequencies [7], is absent in the plateau of the harmonic spectrum. We plot in Fig. 4 the phases of the spectral components $\mathbf{a}_q$. As seen, the harmonics below the cutoff are not phase locked [11]. However, the phase is not completely random. Moreover, the behavior of the frequency dependence of the phase at the end of the plateau is more regular than that at the beginning of the spectrum.

In order to see the effect of the pulse intensity on attosecond pulse generation, we show in Figs. 5 and 6 the numerical results for the cases where the peak intensity of the driver pulse is 5×10^{14} W/cm^2 and 2×10^{15} W/cm^2, respectively. The duration of the driver pulse in both cases is 4 optical cycles. Figures 5(a) and 6(a) show the harmonic emission spectra. A comparison between Figs. 1(a), 5(a), and 6(a) shows that the cutoff energy is higher when the peak intensity of the driver pulse is higher [15,16]. Figures 5(b) and 6(b) show the time dependence of the radiation corresponding to the supercontinuum spectral band between the 72nd and 90th harmonics of the spectrum in Fig. 5(a) and the supercontinuum band between the 244th and 280th harmonics of the spectrum in Fig. 6(a), respectively. The durations of the pulses in Figs. 5(b) and 6(b) are 190 and 110 attoseconds, respectively. When we compare Figs. 2(a), 5(b), and

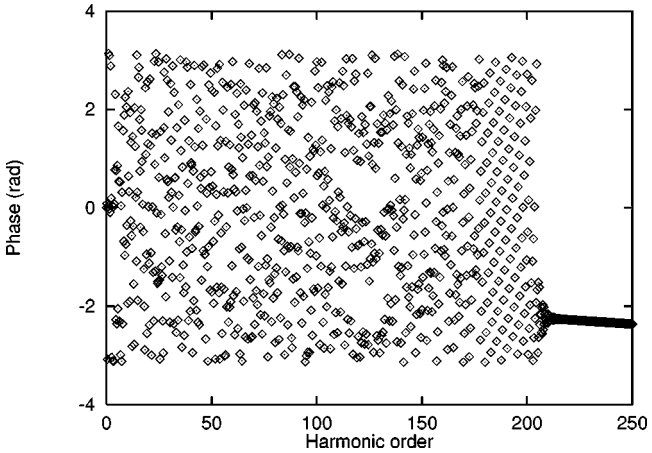

FIG. 4. Phases of the spectral components of the dipole acceleration. All the parameters are the same as for Fig. 1(a).

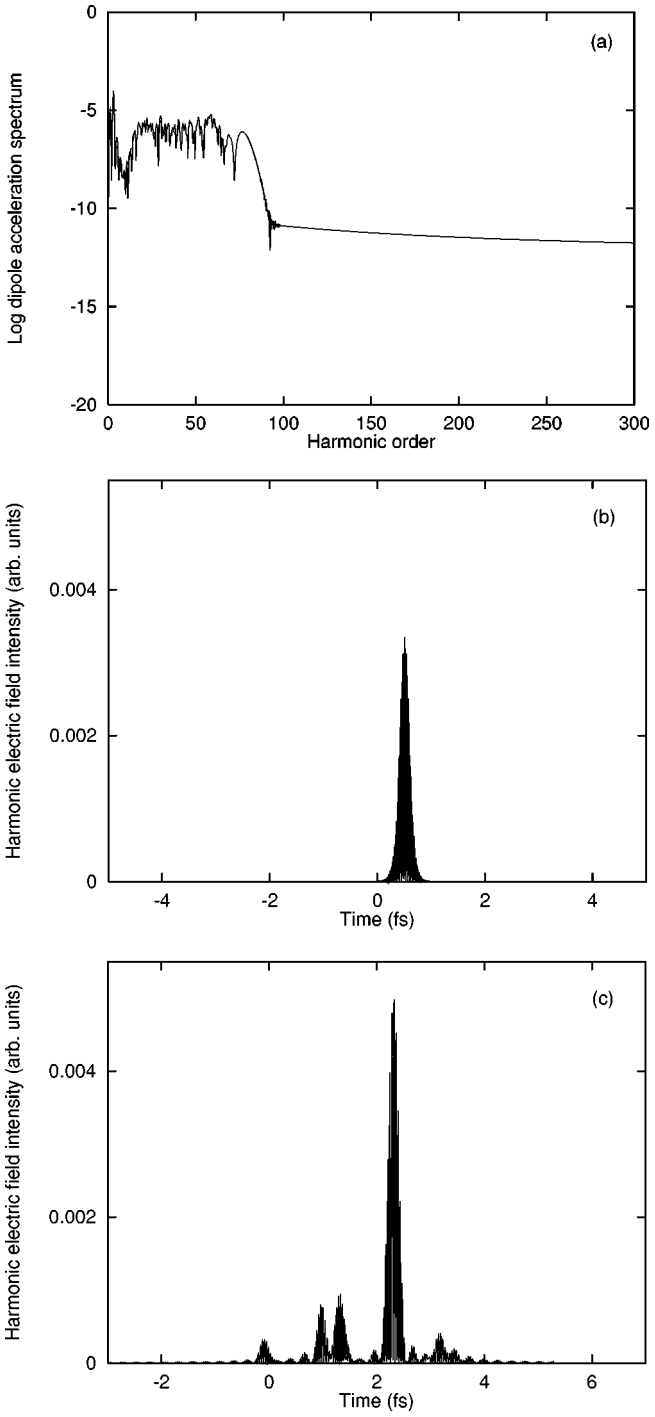

FIG. 5. Harmonic emission in the case when the peak intensity of the driver pulse from the Ti:sapphire laser is 5×10^{14} W/cm^2. The duration of the driver pulse is 4 optical cycles. (a) Power spectral density ($\log_{10}$ scale) of the dipole acceleration. (b) Time dependence of the radiation from the supercontinuum band between the 72nd and 90th harmonics. (c) Time dependence of the radiation from the band between the 30th and 40th harmonics.

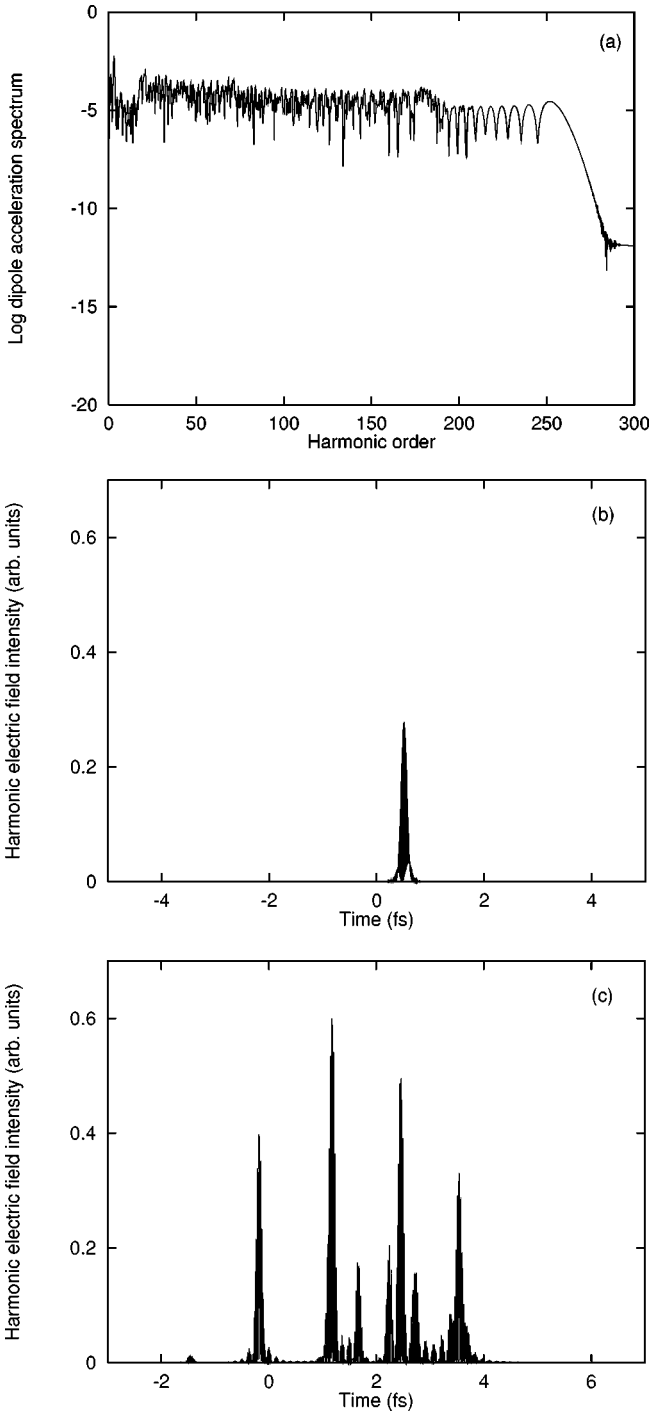

FIG. 6. Harmonic emission in the case when the peak intensity of the driver pulse from the Ti:sapphire laser is 2×10^{15} W/cm^2. The duration of the driver pulse is 4 optical cycles. (a) Power spectral density ($\log_{10}$ scale) of the dipole acceleration. (b) Time dependence of the radiation from the supercontinuum band between the 244th and 280th harmonics. (c) Time dependence of the radiation from the band between the 40th and 60th harmonics.

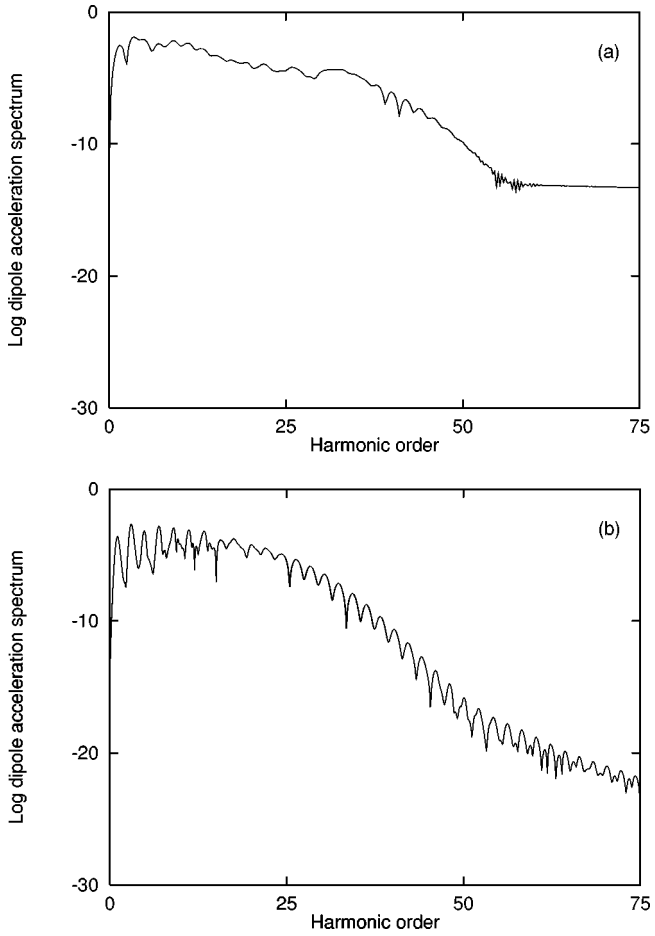

FIG. 7. Power spectral densities ($\log_{10}$ scale) of the dipole acceleration of helium illuminated by the KrF laser field with the wavelength 248 nm and the peak intensity 1×10^{16} W/cm^2. The duration of the driver field is 4 and 16 optical cycles in the cases (a) and (b), respectively.

6(b), we see that the duration of the attosecond pulse corresponding to the supercontinuum spectral band near the end of the plateau is shorter when the peak intensity of the driver pulse is higher. Figures 5(c) and 6(c) show the time dependence of the radiation corresponding to the spectral band between the 30th and 40th harmonics of the spectrum in Fig. 5(a) and the band between the 40th and 60th harmonics of the spectrum in Fig. 6(a), respectively. As seen, trains of attosecond pulses can also be produced by synthesizing the spectral components at the beginnings of the plateaus. However, the behavior of the trains is not as regular as in the case of the supercontinuum bands near the ends of the plateaus.

B. KrF laser driver field

We now use the driver field pulse from the KrF laser. The wavelength and the period of the driver pulse are 248 nm and 0.83 fs, respectively.

We show in Fig. 7 the power spectrum $|\mathbf{a}_q|^2$ in the $\log_{10}$ scale for the case when the peak intensity of the driver pulse is 1×10^{16} W/cm^2. The duration of the driver pulse is 4 (a) and 16 (b) optical cycles. In femtoseconds, the duration of the driver pulse is 3.31 (a) and 13.24 (b) fs. For the chosen parameters, the ionization is substantially complete on the leading edge of the driver pulse, that is, before the pulse intensity reaches its maximum. As seen, the drop of the spectrum from the first few harmonics is not as clear as in the case of the Ti:sapphire laser. The reason is that the quantity I_p/ω corresponding to the harmonic order from which the plateau is expected to start has a small value $I_p/\omega\approx5$ in the case of the KrF laser. Comparison between Figs. 7(a) and 7(b) shows that the cutoff energy is extended towards shorter

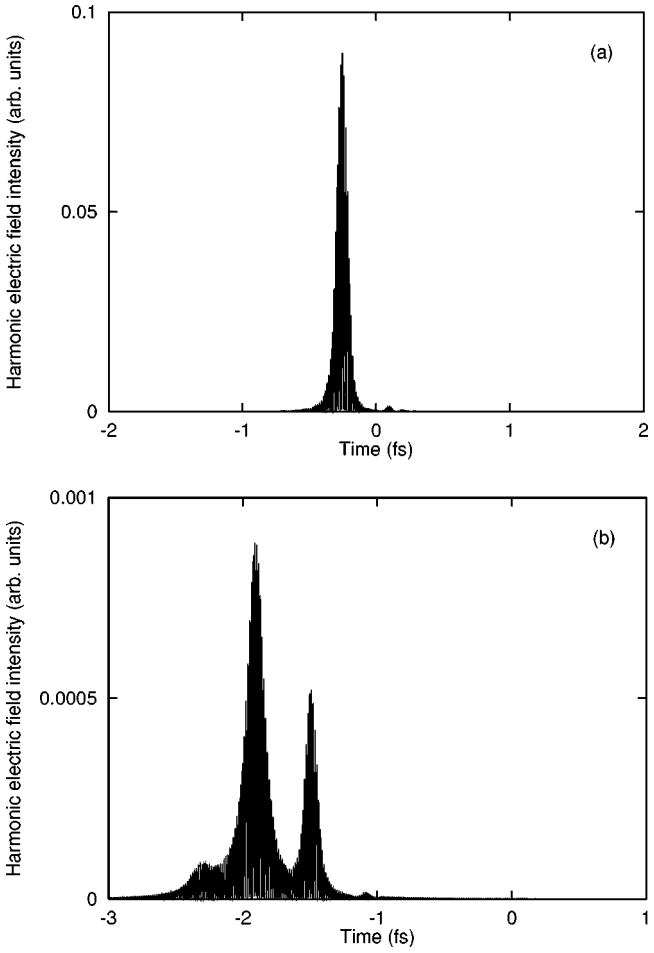

FIG. 8. Time dependencies of the intensities of the superpositions of the spectral components in the bands between the 30th and 40th harmonics of the power spectra in Fig. 7.

wavelengths when the number of optical cycles is decreased [1,4,6]. The reason is that, since the ionization rate is high, the atom can survive higher laser intensity when the pulse duration is shorter. Recently, Chang *et al.* [1] have obtained an interesting analytical expression for the explicit dependence of the cutoff energy on the atomic and laser parameters, which clearly shows that the use of shorter driver pulses should result in the generation of harmonics of higher order.

We plot in Fig. 8 the time dependences of the intensities of the pulses obtained by using a spectral filter to select only the frequency components in the region between the 30th and 40th harmonics, which is relatively regular and near the end of the plateau. Here we again use the relative time calculated from the moment at which the driver pulse reaches its peak. The figures clearly show the generation of single attosecond pulses as well as trains of attosecond pulses, one per half-a-period of the fundamental pulse. The shortest duration of the pulses in the trains is about 100 attoseconds. When we decrease the duration of the driver pulse, the number of attosecond signal pulses in each train decreases and the energy conversion efficiency of the highest pulse increases.

It is also possible to generate attosecond pulses by combining the frequency components which are at the beginning of the plateau. We show in Fig. 9 the time development of

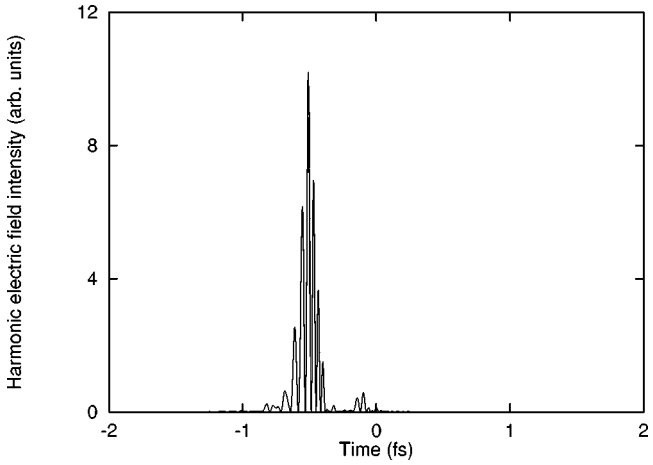

FIG. 9. Time dependence of the intensity of the superposition of the spectral components in the band between the 5th and 15th harmonics of the power spectrum in Fig. 7(a).

the radiation obtained by the Fourier synthesis of the frequency components in the region between the 5th and 15th harmonics of the spectrum in Fig. 7(a). The duration of the generated pulse is approximately 100 attoseconds. Note that the amplitude of this pulse is much higher than that of the pulses obtained in Fig. 8(a), where the synthesis of spectral components between the 30th and 40th harmonics is performed. The reason is very simple: since the effect of atom ionization is weak for the low-order harmonics and strong for the high-order harmonics, the spectral density of the harmonics near the beginning of the plateau is higher than the density of the high harmonics near the end of the plateau. Since the Lewenstein model [17] is a crude approximation in the region of low-order harmonics, there may be some differences between the results of this model and the exact numerical solution of the Schrödinger equation. However, we expect that these differences do not change our principal statement about the possibility of trains of attosecond pulses in the low-order harmonic region. The main reason is that the Coulomb potential is not completely neglected in the Lewenstein model. For the KrF laser, there is another reason: the photon energy and, consequently, the energies of harmonics of this laser are high.

We show in Figs. 10 and 11 the numerical results for the cases where the peak intensity of the driver pulse is 5×10^{15} W/cm^2 and 1.5×10^{16} W/cm^2, respectively. The duration of the driver pulse in both cases is 4 optical cycles. Figures 10(a) and 11(a) show the harmonic emission spectra. Figures 10(b) and 11(b) show the time dependence of the radiation corresponding to the supercontinuum spectral band between the 23rd and 30th harmonics of the spectrum in Fig. 10(a) and the supercontinuum band between the 40th and 60th harmonics of the spectrum in Fig. 11(a), respectively. The durations of the pulses in Figs. 10(b) and 11(b) are 150 and 80 attoseconds, respectively. When we compare Figs. 8(a), 10(b), and 11(b), we see that the duration of the attosecond pulse corresponding to the supercontinuum spectral band near end of the plateau is shorter when the peak intensity of the driver pulse is higher. Figures 10(c) and 11(c) show the time dependence of the radiation corresponding to the spectral band between the 7th and 15th harmonics of the spectrum in Fig. 10(a) and the band between the 7th and 15th

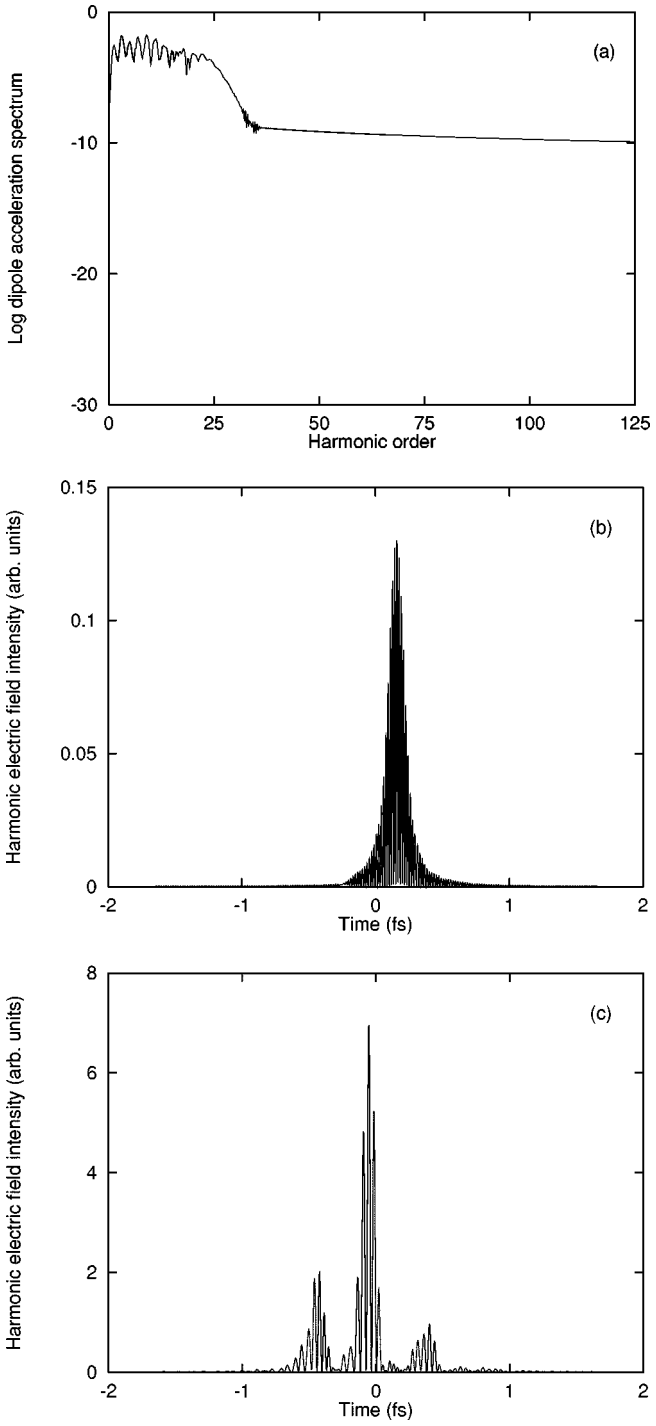

FIG. 10. Harmonic emission in the case when the peak intensity of the driver pulse from the KrF laser is 5×10^{15} W/cm^2. The duration of the driver pulse is 4 optical cycles. (a) Power spectral density ($\log_{10}$ scale) of the dipole acceleration. (b) Time dependence of the radiation from the supercontinuum band between the 23rd and 30th harmonics. (c) Time dependence of the radiation from the band between the 7th and 15th harmonics.

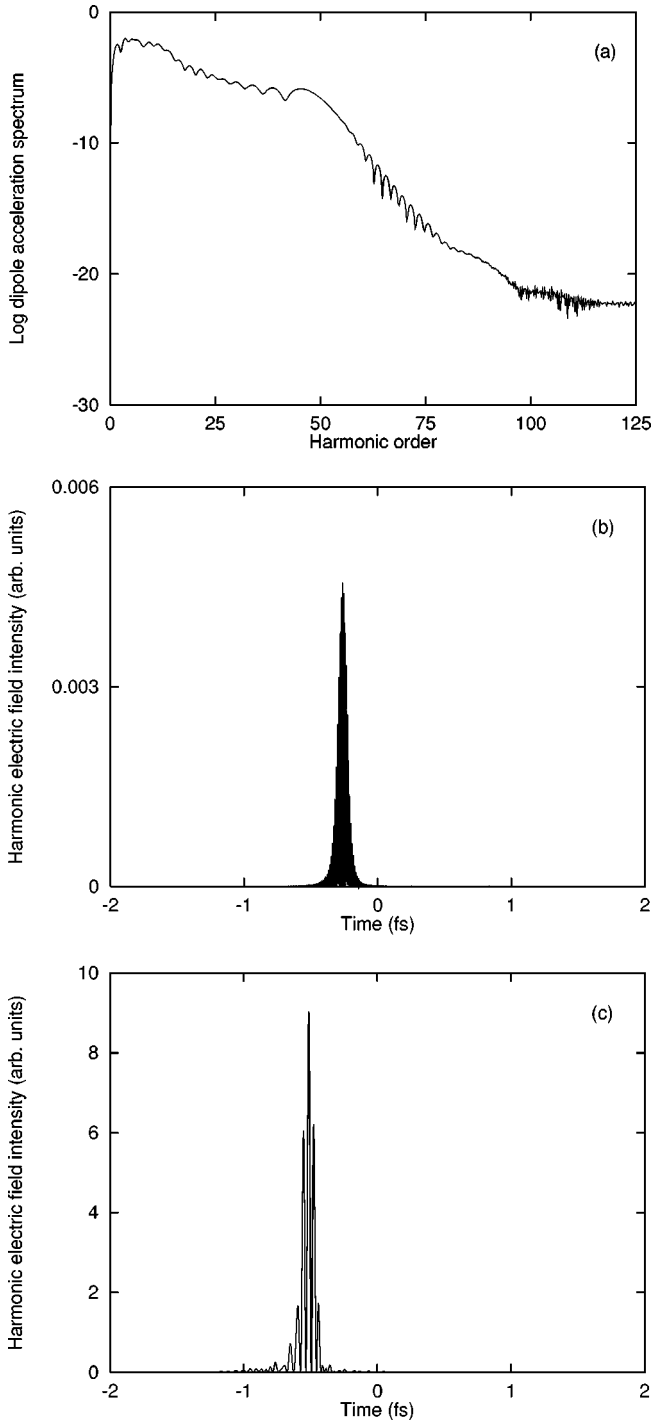

FIG. 11. Harmonic emission in the case when the peak intensity of the driver pulse from the KrF laser is 1.5×10^{16} W/cm^2. The duration of the driver pulse is 4 optical cycles. (a) Power spectral density ($\log_{10}$ scale) of the dipole acceleration. (b) Time dependence of the radiation from the supercontinuum band between the 40th and 60th harmonics. (c) Time dependence of the radiation from the band between the 7th and 15th harmonics.

harmonics of the spectrum in Fig. 11(a), respectively. As seen, trains of attosecond pulses can also be produced by synthesizing the spectral components at the beginnings of the plateaus. However, the behavior of the trains is not as regular as in the case when the spectral band for synthesis is near the end of the plateau.

IV. CONCLUSIONS

We have studied the generation of high harmonics from He atoms illuminated by high-intensity femtosecond excitation pulses from the Ti:sapphire and KrF lasers. We have shown that by performing the Fourier synthesis of the spectral components that are near the end of the plateau, single

attosecond pulses as well as trains of several attosecond pulses, one per half a period, can be generated in the multicycle regime of the driver pulse. For the parameters of the calculations, the shortest durations of the pulses in the trains are found to be about 110 attoseconds in the case of the Ti:sapphire laser and 80 attoseconds in the case of the KrF laser. We have shown that the number of attosecond high-harmonic pulses in each train decreases and the energy conversion efficiency of the highest pulse in the train increases when we decrease the number of optical cycles of the driver field. It is also possible to generate attosecond pulses by combining the frequency components in the bands which are positioned at the beginning of the spectrum or in front or middle of the plateau. However, the behavior of the optical oscillations of the pulses obtained in this way is less regular than the behavior of the pulses generated by the synthesis of the spectral components in the bands which are near the end of the plateau. Furthermore, we have shown that the duration of the attosecond pulse corresponding to the supercontinuum spectral band, which is near to end of the plateau, is shorter when the peak intensity of the driver pulse is higher.

Practical consideration of the high-harmonic generation process requires an understanding of propagation effects, which have not been addressed in this paper. In order to study such effects, one needs to solve the wave equations, using the dipole moments as source terms. One may anticipate that the intensity dependence of the phase of the dipole moment has a strong influence on the propagation and can lead to strong spatial distortion as well as spectral broadening. However, the coherence of the harmonics can be controlled and optimized by choosing appropriately the geometry of the interaction and the position of the laser focus relative to the nonlinear medium. In addition, the phase mismatch due to focusing can be ameliorated by making the gas target thin. A special analysis of the effect of propagation on the durations and coherent properties of the generated pulses will be the subject of a future work. Furthermore, since the Lewenstein model is a crude approximation in the region of low-order harmonics, an additional study involving the exact numerical solution of the Schrödinger equation will be required for the attosecond pulses from this region of the harmonic spectrum.

[1] Z. Chang, A. Rundquist, H. Wang, M. M. Murnane, and H. C. Kapteyn, Phys. Rev. Lett. **79**, 2967 (1997).
[2] Ch. Spielmann, N. H. Burnett, S. Sartania, R. Koppitsch, M. Schnürer, C. Kan, M. Lenzner, P. Wobrauschek, and F. Krausz, Science **278**, 661 (1997).
[3] A. Bouhal, R. Evans, G. Grillon, A. Mysyrowicz, P. Breger, P. Agostini, R. C. Constantinescu, H. G. Muller, and D. von der Linde, J. Opt. Soc. Am. B **14**, 950 (1997).
[4] I. P. Christov, J. Zhou, J. Peatross, A. Rundquist, M. M. Murnane, and H. C. Kapteyn, Phys. Rev. Lett. **77**, 1743 (1996).
[5] P. Salières, A. L'Huillier, and M. Lewenstein, Phys. Rev. Lett. **74**, 3776 (1995).
[6] C. Kan, N. H. Burnett, C. E. Capjack, and R. Rankin, Phys. Rev. Lett. **79**, 2971 (1997).
[7] T. W. Hänsch, Opt. Commun. **80**, 71 (1990).
[8] Gy. Farkas and Cs. Tóth, Phys. Lett. A **168**, 447 (1992).
[9] S. E. Harris, J. J. Macklin, and T. W. Hänsch, Opt. Commun. **100**, 487 (1993).
[10] P. B. Corkum, N. H. Burnett, and M. Y. Ivanov, Opt. Lett. **19**, 1870 (1994).
[11] P. Antoine, A. L'Huillier, and M. Lewenstein, Phys. Rev. Lett. **77**, 1234 (1996).
[12] K. J. Schafer and K. C. Kulander, Phys. Rev. Lett. **78**, 638 (1997).
[13] I. P. Christov, M. M. Murnane, and H. C. Kapteyn, Phys. Rev. Lett. **78**, 1251 (1997).
[14] P. Antoine, D. B. Milošević, A. LHuillier, M. B. Gaarde, P. Salières, and M. Lewenstein, Phys. Rev. A **56**, 4960 (1997).
[15] P. B. Corkum, Phys. Rev. Lett. **71**, 1994 (1993).
[16] K. C. Kulander, K. J. Schafer, and J. L. Krause, in *Super Intense Laser-Atom Physics*, Vol. 316 of *NATO Advanced Studies Institute Series B: Physics*, edited by B. Piraux *et al.* (Plenum, New York, 1993).
[17] M. Lewenstein, Ph. Balcou, M. Yu. Ivanov, A. L'Huillier, and P. B. Corkum, Phys. Rev. A **49**, 2117 (1994).
[18] M. V. Ammosov, N. B. Delone, and V. P. Krainov, Zh. Eksp. Teor. Fiz. **91**, 2008 (1986) [Sov. Phys. JETP **64**, 1191 (1986)].